

Mathematical Modeling on Capturing of Magnetic Nanoparticles in an Implant Assisted Channel for Magnetic Drug Targeting

Shashi Sharma, V. K. Katiyar, Uday Singh

Abstract—In IA-MDT, the magnetic implants are placed strategically at the target site to greatly and locally increase the magnetic force on MDCPs and help to attract and retain the MDCPs at the targeted region. In the present work, we develop a mathematical model to study the capturing of magnetic nanoparticles flowing within a fluid in an implant assisted cylindrical channel under magnetic field. A coil of ferromagnetic SS-430 has been implanted inside the cylindrical channel to enhance the capturing of magnetic nanoparticles under magnetic field. The dominant magnetic and drag forces, which significantly affect the capturing of nanoparticles, are incorporated in the model. It is observed through model results that capture efficiency increases as we increase the magnetic field from 0.1 to 0.5 T, respectively. The increase in capture efficiency by increase in magnetic field is because as the magnetic field increases, the magnetization force, which is attractive in nature and responsible to attract or capture the magnetic particles, increases and results the capturing of large number of magnetic particles due to high strength of attractive magnetic force.

Keywords—Capture efficiency, Implant assisted-Magnetic drug targeting (IA-MDT), Magnetic nanoparticles (MNP).

I. INTRODUCTION

THE ability to manipulate magnetic particles in fluid flows by means of inhomogeneous magnetic fields is used in a wide range of biomedical applications including magnetic drug targeting (MDT). Magnetic drug targeting (MDT) is a therapeutic technique that uses an external magnetic field to retain magnetic drug carrier particles (MDCPs) at the region of interest to avoid full circulation in human body, reduce the curing time, and minimize dosages and side effects. Sufficient introductory and background information on MDT can be found in [1] and [2], among many others. The concept of MDT has been around for many years [3], [4]; however, this technique is still looming despite the fact that it has shown some promise in both *in vivo* [5]–[7] and clinical [8], [9] studies.

Compared with traditional chemotherapy, the accumulation and retention of the magnetic drug carrier particles can be improved by using an external magnetic field, which is focused on the area of the tumour. Many studies have shown that MDT is relatively safe and effective methodology for targeting drugs to a specific site in the body [10]–[12]. However, there are two major limitations of MDT. Firstly,

MDCP retention is quite low due to weak magnetic forces which are not always strong enough to overcome fluidic drag forces. The second limitation is the depth of the targeted site within the body; MDT is mostly favorable in tropical regions near the skin since the magnetic forces decay with distance. Even in the most favorable situation, studies have shown that it is difficult to collect appreciable amounts of the MDCPs at the target site [6], [8]. To overcome these limitations of the traditional MDT approach, [12]–[16] reported the implant assisted magnetic drug targeting (IA-MDT).

In IA-MDT, the magnetic implants are placed at the target site to greatly and locally increase the magnetic force on MDCPs which help to attract and retain the MDCPs at the targeted region [17], [18]. This implant assisted MDT approach has been studied theoretically [12], [13], [16], [17], [19] as well as experimentally by many researchers [14], [16]–[18]. Initially, the concept of IA-MDT was reported by [12] followed by different studies using various types of implants. Chen et al. [20] theoretically evaluated the IA-MDT of drug encapsulated nanoparticles using intravascular stent, while *in vitro* experiments have evaluated the IA-MDT using ferromagnetic stents by [22] and [17]. Cregg et al. [21] extended the theoretical study of [20] by incorporating the superparamagnetic property of MDCPs and determined their magnetic moment using the Langevin function. Thus IA-MDT is very effective to improve the capture efficiency of ferromagnetic nanoparticles through implanting a ferromagnetic coil as stent inside the simulated blood vessel.

In view of above, a mathematical model is presented to study the capture efficiency of iron oxide magnetic nanoparticles transported in a ferromagnetic SS-430 coil implanted cylindrical tube (simulated blood vessel). The obtained results show that the capture efficiency increases by increasing the magnetic field and decreases as inlet velocity increases.

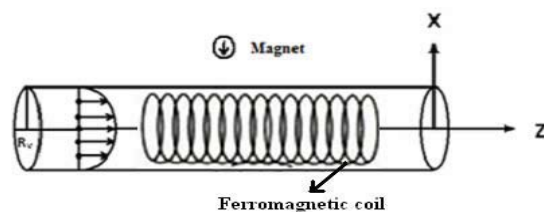


Fig. 1 Schematic geometry of the magnetic particles transported in a cylindrical tube implanted with a ferromagnetic coil. The source magnet is positioned outside the tube to apply the magnetic field.

II. DESCRIPTION AND FORMULATION OF THE PROBLEM

A. Description of the Problem

A mathematical model is developed to calculate the capture efficiency of magnetic nanoparticles flowing within fluid in an implanted cylindrical tube (simulated blood vessel) with ferromagnetic stainless steel (SS-430) coil under magnetic field. The magnetic nanoparticles are injected into a blood vessel and their flow within artificial blood (in the z-direction along the axis of blood vessel) is targeted by applying an external magnetic field. The magnetic field is applied by a magnet positioned outside the tube. The magnet is assumed to be infinite extent and oriented to the perpendicular direction of the blood flow (x-direction). The schematic diagram of magnetic particles transported in a cylindrical tube implanted with a ferromagnetic coil is depicted in Fig. 1. The blood vessel is assumed to be a cylindrical tube with laminar flow of magnetic particles within blood parallel to its axis.

B. Mathematical Formulation

There are various forces such as magnetic force, viscous drag force, particle-particle interaction, particle-fluid interaction, buoyancy, and gravitational force which affect the motion of magnetic particles in a fluid under the influence of applied external magnetic field. In the present study, we consider only the dominant magnetization and viscous drag forces and all other forces are neglected.

C. Magnetic Force:

The magnetic force is given by

$$\mathbf{F}_m = \mu_0 V_p (\mathbf{M} \cdot \nabla) \mathbf{H}_{total} \quad (1)$$

where V_p is the volume, \mathbf{M} is the magnetization of the particle, $\mu_0 = 4\pi \times 10^{-7} \text{ NA}^{-2}$ is the magnetic permeability of free space, and \mathbf{H}_{total} is the total field exerted on the magnetic particles. In the present geometry, a magnetizable stent coil is inserted inside the cylindrical tube as shown in Fig. 1. This ferromagnetic stent coil got magnetized under the influence of external magnetic field then total magnetic field \mathbf{H}_{total} experienced by magnetic particles can be written as

$$\mathbf{H}_{total} = \mathbf{H} + \mathbf{M}_{stent} \quad (2)$$

where \mathbf{M}_{stent} is the induced magnetization of the stent coil. A magnetizable stent coil, which is placed perpendicular to the applied field direction induced the magnetization (\mathbf{M}_{stent}) parallel to the direction of external magnetic field (\mathbf{H}) and can be calculated as [12]

$$\mathbf{M}_{stent} = 2\alpha_{stent} \mathbf{H} \quad (3)$$

where α_{stent} is the demagnetization factor for cylindrical magnetized stent coil placed perpendicular to the magnetic field direction and approximately given by [12]

$$\alpha_{stent} = \min \left(\frac{\chi_{stent,0}}{2 + \chi_{stent,0}}, \frac{M_{stent,s}}{2|\mathbf{H}_s|} \right) \quad (4)$$

where $\chi_{stent,0}$ is the magnetic susceptibility of the stent coil at zero magnetic field, $M_{stent,s}$ is the saturation magnetization of stent coil and \mathbf{H}_s is the saturation magnetic field. Then value of α_{stent} can be calculated as

$$\alpha_{stent} = \frac{M_{stent,s}}{2|\mathbf{H}_s|} \quad (5)$$

The value of saturation magnetization of ferromagnetic SS-430 stent coil is taken from magnetization versus field ($M-H$) curves reported by [22]. It is observed by this curve that the value of saturated magnetization of stent coil ($M_{stent,s}$) is 1261 kA/m at 1 Tesla (797700 A/m) field. By using this data in (5), the value of α_{stent} is found 0.79 for ferromagnetic SS-430 stent. Then, the value of \mathbf{M}_{stent} can be calculated by putting $\alpha_{stent} = 0.79$ in (3):

$$\mathbf{M}_{stent} = 2\alpha_{stent} \mathbf{H} = 1.58\mathbf{H} \quad (6)$$

Equation (6) shows that the ferromagnetic stent coil exerts 1.58 \mathbf{H} magnetic field on magnetic particles in addition to applied field \mathbf{H} . Therefore, as per (2), the total magnetic field experienced by magnetic particles will be as:

$$\mathbf{H}_{total} = \mathbf{H} + 1.58\mathbf{H} = 2.58\mathbf{H} \quad (7)$$

Then magnetic force experienced by magnetic particles in a ferromagnetic stainless steel (SS-430) implanted cylindrical tube is given by

$$\mathbf{F}_m = \mu_0 V_p (\mathbf{M} \cdot \nabla) (2.58\mathbf{H}) \quad (8)$$

D. Viscous Drag Force

The viscous drag force, which is obtained by Stokes' Drag approximation

$$\mathbf{F}_D = 6\pi\mu_f R_p (\mathbf{v}_f - \mathbf{v}_p), \quad \text{Re}_p \ll 1 \quad (9)$$

where \mathbf{v}_f and \mathbf{v}_p are the velocities of the fluid and particle, respectively. μ_f is the viscosity of fluid.

E. Equations of Motion

The motion of the particle in fluid can be described by Newton's Law:

$$m_p \frac{d\mathbf{v}_p}{dt} = \mathbf{F}_m + \mathbf{F}_D \quad (10)$$

where m_p is the mass of the particles. The inertial term is very small and could be ignored. Then (10) can be written as:

$$\mathbf{F}_m + \mathbf{F}_D = 0 \quad (11)$$

The equation of motion in axial direction is given by

$$\frac{dz}{dt} = \frac{F_{mz}}{6\pi\mu_f R_p} + u_0 \left(1 - \frac{x^2}{R_v^2}\right) \quad (12)$$

and in vertical direction is

$$\frac{dx}{dt} = \frac{F_{mx}}{6\pi\mu_f R_p} \quad (13)$$

F. Capture Efficiency

The capture efficiency of magnetic particles is defined as the ratio between the total number of particles captured along the vessel walls and the total number of released particles.

$$\eta = \frac{n_{in} - n_{out}}{n_{in}} = \frac{1 - \bar{x}_0}{2} \quad (14)$$

where n_{in} and n_{out} are the number of particle entering and leaving the vessel. After solving (8), (9), (11)-(14), the following formula for capture efficiency is observed,

$$\eta = \frac{1}{3} R_p \sqrt{\frac{2\mu_0 M H_{total}}{R_v \mu_f u_0}} \quad (15)$$

H_{total} is 2.58 times of external magnetic field (H). So, (15) can be written as

$$\eta = \frac{1}{3} R_p \sqrt{\frac{2\mu_0 M (2.58) H}{R_v \mu_f u_0}} \quad (16)$$

The formula represented by (16) shows that the capture efficiency for the ferromagnetic SS-430 stent coil increases $\sqrt{2.58} = 1.6$ times as compared to without stent geometry.

In this study, the iron oxide (Fe_3O_4) particles of radius ($R_p = 300$ nm) are taken into account as magnetic nanoparticles with density $\rho_p = 5000$ kg/m³. Further, a rare earth NdFeB cylindrical magnet was used to apply the magnetic field positioned outside the body with its saturation

magnetization of 10^6 A/m. The radius of blood vessel (R_v) is selected 3 mm and the inlet flow velocity (u_0) is varied from 2-8 mm/s. The viscosity (μ_f) of the blood is assumed to be 3.2×10^{-3} N s/m². A ferromagnetic SS-430 coil of diameter 5 mm with saturated magnetization of ($M_{stent,s}$) 1261 kA/m at 1 Tesla (797700 A/m) field is used as a stent coil placed inside the blood vessel.

III. RESULTS AND DISCUSSION

The capture efficiency (η) of magnetic particles with magnetic fields (0-0.5 T) at various inlet velocities is shown in Fig. 2. The curve indicates that capture efficiency increases from 36 to 81 % by increasing magnetic field from 0.1 to 0.5 Tesla, respectively for $u_0 = 2$ mm/s. The increase in capture efficiency with magnetic field is because as the magnetic field increases, the magnetization force, which is attractive in nature and responsible to attract or capture the magnetic particles, increases and results the capture of large number of magnetic particles due to high strength of attractive magnetic force. These values of capture efficiency are 1.6 times larger to the capture efficiencies calculated for without stent geometry. This is because under the influence of external magnetic implanted, stent becomes magnetized and creates its own magnetic field around itself along with external magnetic field, which is 1.58 times of external magnetic field as represented. The presence of stent also distorts the external magnetic field creating large gradient. Both of these changes in local magnetic field around the implanted stent increase the force exerted on MDCPs that are traveling in the vicinity of the stent, which in turn results the enhancement in retention of MDCPs as well as capture efficiency.

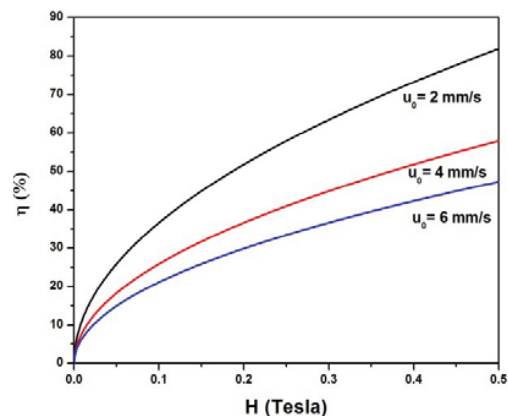


Fig. 2 Model results of capture efficiency (η) versus magnetic fields at different inlet velocities (u_0) for implant assisted cylindrical tube

The capture efficiency (η) of magnetic particles with inlet velocities (2-8 mm/s) at different magnetic fields is shown in Fig. 3. The curve indicates that capture efficiency decreases from 81 to 41 % as we increase the inlet velocities from 2 to 8 mm/s, respectively at $H = 0.5$ Tesla. These values of capture

efficiency are 1.6 times larger than the capture efficiencies calculated for without stent geometry due to enhanced magnetic force on MDCPs by the presence of ferromagnetic stent. The decrease in capture efficiency with inlet velocity is due to dominance of hydrodynamic drag force over magnetic force at higher inlet velocities, which results the reduction in capture efficiency. Moreover, at the higher flow velocities, MDCPs get less time to enter in the capture region and have the higher chance to be flushed away.

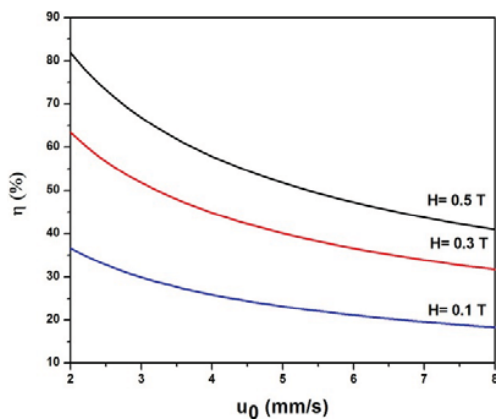


Fig. 3 Model results of capture efficiency (η) versus inlet velocities at different magnetic fields (H) for implant assisted cylindrical tube

IV. CONCLUSIONS

In summary, a mathematical model is presented to study the effect of magnetic field and inlet velocity on capture efficiency by including dominant magnetization and drag forces. Model results show that capture efficiency increases from 36 to 81% as we increase the magnetic field from 0.1 to 0.5 T, respectively. The increase in capture efficiency by increase in magnetic field is because as the magnetic field increases, the magnetization force, which is attractive in nature and responsible to attract or capture the magnetic particles, increases and results the capturing of large number of magnetic particles due to high strength of attractive magnetic force. However, decrease in capture efficiency is noticed from 81 to 41% by increasing the inlet velocity from 2 to 8 mm/s, respectively.

REFERENCES

- [1] U. O. Häfeli, "Magnetically modulated therapeutic systems." *Int. J. pharm.*, Vol. 277(1), 2004, pp. 19-24.
- [2] C. Alexiou, R. Jurgons, Magnetic drug targeting. In: Magnetism in medicine: a handbook, 2nd edn. 2007 pp. 596-605
- [3] K. J. Widder, A. E. Senyei, & D. G. Scarpelli, "Magnetic microspheres: a model system for site specific drug delivery *in vivo*." *Exp Biol Med*, Vol. 158(2), 1978, pp. 141-146.
- [4] A. Senyei, K. Widder, & G. Czerlinski, (1978). "Magnetic guidance of drug-carrying microspheres." *J. Appl Phys*, Vol. 49(6), 1978, pp. 3578-3583.
- [5] C. Alexiou, W. Arnold, R. J. Klein, R. F. G. Parak, P. Hulin, C. Bergemann, & A. S. Luebbe, "Locoregional cancer treatment with magnetic drug targeting." *Cancer Res*, Vol. 60(23), 2000, pp. 6641-6648.
- [6] H. Xu, T. Song, X. Bao & L. Hu, "Site-directed research of magnetic nanoparticles in magnetic drug targeting." *J. magn. Magn. Mater*, Vol. 293(1), 2005, pp. 514-519.

- [7] C. Alexiou, R. J. Schmid, R. Jurgons, M. Kremer, G. Wanner, C. Bergemann, & F. G. Parak, "Targeting cancer cells: magnetic nanoparticles as drug carriers." *Eur Biophys J*. Vol. 35(5), 2006, pp. 446-450.
- [8] A. S. Lübbe, C. Bergemann, J. Brock, & D. G. McClure. "Physiological aspects in magnetic drug-targeting." *J. magn. Magn. Mater*, Vol. 194(1), 1999, pp. 149-155.
- [9] A. S. Lübbe, C. Alexiou, & C. Bergemann, "Clinical applications of magnetic drug targeting." *J. Surg. Res*, Vol. 95(2), 2001, pp. 200-206.
- [10] M. O. Avilés, A. D. Ebner, J.A. & Ritter. "In vitro study of magnetic particle seeding for implant assisted-magnetic drug targeting." *J. magn. Magn. Mater* Vol. 320(21), 2008, pp. 2640-2646.
- [11] M. O. Avilés, A. D. Ebner, & J. A. Ritter, "In vitro study of magnetic particle seeding for implant-assisted-magnetic drug targeting: Seed and magnetic drug carrier particle capture." *J. magn. Magn. Mater*, Vol. 321(10), 2009, pp. 1586-1590.
- [12] J. A. Ritter, A. D. Ebner, K. D. Daniel, & K. L. Stewart, "Application of high gradient magnetic separation principles to magnetic drug targeting." *J. magn. Magn. Mater*, Vol. 280(2), 2004, pp. 184-201.
- [13] M. O. Avilés, A. D. Ebner, H. Chen, A. J. Rosengart, M. D. Kaminski, & J. A. Ritter. "Theoretical analysis of a transdermal ferromagnetic implant for retention of magnetic drug carrier particles." *J. magn. Magn. Mater*, Vol. 293(1), 2005, pp. 605-615.
- [14] M. O. Avilés, A. D. Ebner, & J. A. Ritter. "Ferromagnetic seeding for the magnetic targeting of drugs and radiation in capillary beds." *J. magn. Magn. Mater*, Vol. 310(1), 2007, pp. 131-144.
- [15] O. Rotariu, & N. J. Strachan. "Modelling magnetic carrier particle targeting in the tumor microvasculature for cancer treatment." *J. magn. Magn. Mater*, Vol. 293(1), 2005, pp. 639-646.
- [16] B. B. Yellen, Z. G. Forbes, D. S. Halverson, G. Fridman, K.A. Barbee, M. Chorny & G. Friedman. "Targeted drug delivery to magnetic implants for therapeutic applications." *J. magn. Magn. Mater*, Vol. 293(1), 2005, pp. 647-654.
- [17] Z. G. Forbes, B. B. Yellen, K. Barbee, & G. Friedman. "An approach to targeted drug delivery based on uniform magnetic fields." *Magnetics, IEEE Transactions on*, Vol. 39(5), 2003, pp. 3372-3377.
- [18] J. O. Mangual, M.O. Avilés, A. D. Ebner, & J. A. Ritter. "In vitro study of magnetic nanoparticles as the implant for implant assisted magnetic drug targeting." *J. magn. Magn. Mater*, Vol. 323(14), 2011, pp. 1903-1908.
- [19] K. Hourmumnuard, & M. Natenapit. "Magnetic drug targeting by ferromagnetic microwires implanted within blood vessels." *Med. Phys*, Vol. 40(6), 2013, pp. 062302.
- [20] H. Chen, A. D. Ebner, M. D. Kaminski, A. J. Rosengart, J. A. Ritter. "Analysis of magnetic drug carrier particle capture by a magnetizable intravascular stent—2: parametric study with multi-wire two-dimensional model." *J Magn Magn Mater*, Vol. 293(1), 2005, pp. 616-632
- [21] P. J. Cregg, K. Murphy, & A. Mardinoglu. "Calculation of nanoparticle capture efficiency in magnetic drug targeting." *J. magn. Magn. Mater*, Vol. 320(23), 2008, pp. 3272-3275.
- [22] M. O. Avilés, A. D. Ebner, & J. A. Ritter. "Implant assisted-magnetic drug targeting: comparison of *in vitro* experiments with theory." *J. magn. Magn. Mater*, Vol. 320(21), 2008, pp. 2704-2713.